processes

MDPI

Article

Multi-Type Energy Storage Collaborative Planning in Power System Based on Stochastic Optimization Method

Yinguo Yang [1], Qiuyu Lu [1], Zhenfan Yu [1], Weihua Wang [1] and Qianwen Hu [2,*]

[1] Guangdong Power Grid Dispatch and Control Center, Guangzhou 510600, China; yangyinguo@gddd.csg.cn (Y.Y.); luqiuyu0708@gdpc.gd.csg.cn (Q.L.); yuzhenfan@gpdc.gd.csg.cn (Z.Y.); wangweihua@gdpc.gd.csg.cn (W.W.)

[2] State Key Laboratory of Electrical Insulation and Power Equipment, Xi'an Jiaotong University, Xi'an 710049, China

* Correspondence: qwhu089@stu.xjtu.edu.cn

Abstract: As the proportion of renewable energy in power system continues to increase, that power system will face the risk of a multi-time-scale supply and demand imbalance. The rational planning of energy storage facilities can achieve a dynamic time–delay balance between power system supply and demand. Based on this, and in order to realize the location and capacity optimization determination of multiple types of energy storage in power system, this paper proposes a collaborative optimization planning framework for multiple types of energy storage. The proposed planning framework is modelled as a two-stage MILP model based on scenarios via the stochastic optimization method. In the first stage, investment decisions are made for two types of energy storage: battery energy storage (short term) and hydrogen energy storage (long term). In the second stage, power system operation simulation is conducted based on typical scenarios. Finally, the progressive hedging (PH) algorithm is applied to realize the efficient solving of the proposed model. A modified IEEE 39-bus test system is used to verify the validity of the proposed multiple types of energy storage collaborative optimization planning model and PH algorithm.

Keywords: multi-type energy storage; optimization planning; power system; stochastic optimization

Citation: Yang, Y.; Lu, Q.; Yu, Z.; Wang, W.; Hu, Q. Multi-Type Energy Storage Collaborative Planning in Power System Based on Stochastic Optimization Method. *Processes* **2024**, *12*, 2079. https://doi.org/10.3390/pr12102079

Academic Editors: Dawei Zhao, Junyi Zhai, Shengyuan Liu and Wangqianyun Tang

Received: 15 August 2024
Revised: 21 September 2024
Accepted: 22 September 2024
Published: 25 September 2024

1. Introduction

The need to develop renewable energy in order to achieve net zero carbon emissions has become a consensus of all of the countries in the world [1]. However, renewable energy source (RES) output is significantly influenced by weather conditions. As the proportion of RES continues to increase, power system will face the risk of a mismatch between supply and demand on multiple time scales due to the uncertainty of the RES output. Specifically, the fluctuation of RES output can cause the net load curve to become a "canyon curve" in some areas [2], with the seasonal mismatch between RES and load leading to a seasonal imbalance between supply and demand [3]. The uncertainty of RES brings a great challenge to the balance of supply and demand of power system. Under this context, energy storage technology is considered both an important technology and a key form of equipment with which to address the challenge of balancing supply and demand over multiple time scales in power system with a high proportion of RES access. However, the presence of only one single type of energy storage resource is not enough to address the balance of supply and demand on multiple time scales [4]. The coordination of multiple types of energy storage is needed to achieve the dynamic time–delay balance of supply and demand and to adapt to the uncertainty of RES output. Among various energy storage technologies, the flexibility and rapid response of battery energy storage make it an indispensable part of a power system. In addition, hydrogen energy storage is regarded as a key technology with which to achieve deep decarbonization and long-term energy storage, especially in seasonal energy storage applications. The development of battery energy storage and

hydrogen energy storage technologies will play a key role in achieving climate change goals [5]. According to the IEA forecast, by 2030, the installed capacity of global energy storage, including hydrogen energy storage, battery energy storage, etc., needs to reach about 1000 gigawatts (GW) in order to meet the climate goals and energy transition needs of countries [6]. Therefore, the need to study the collaborative planning method of multi-type energy storage systems (MESS), in order to realize the optimal allocation of multiple types of energy storage, is of great significance.

There are many studies that have examined planning methods for ESS. For battery energy storage planning, [7] considers the uncertainty of RES, and a robust optimization model is adopted to optimize the configuration of battery energy storage on the RES side. Based on the principle of equal area, [8] optimizes the battery energy storage capacity from the perspective of the efficient consumption of RES. In [9], considering the uncertainty of RES and from the perspective of improving the flexibility of power system, a distributionally robust optimization model is established for battery energy storage configuration. However, the planning result obtained by robust optimization is too conservative, which makes the economy of the planning scheme poor [10]. It is necessary to further improve the economy of the planning scheme through stochastic optimization methods and consider the influence of RES uncertainties. In addition, there is much research that has studied the planning of hydrogen energy storage. Ref. [11] proposes a hydrogen energy storage optimization model. Ref. [12] proposes a hydrogen energy storage planning model which considers the physical characteristics of hydrogen energy storage. Ref. [13] models hydrogen energy storage systems by Simulink. Ref. [14] models a hydrogen storage system and proposes an electricity–heat–hydrogen optimization operation model. Based on these studies, some research has studied the collaborative planning methods of MESS. Ref. [15] analyses hydrogen energy storage and battery energy storage capacity by seasonal–trend decomposition using LOESS (STL) decomposition technology. Ref. [16] formulates a hydrogen energy storage model and incorporates it in the co-planning model of power system to realize hydrogen energy storage and battery energy storage planning. Ref. [17] proposes a hybrid hydrogen–battery storage planning model for microgrids, where the hydrogen–battery operation constraints are modelled and the planning model is formulated as a scenario-based two-stage model. Ref. [18] proposes a joint optimization planning model of a hydrogen-based carbon-free microgrid including hydrogen energy storage and battery energy storage and is formulated as a convex relaxation-based planning model. Ref. [19] proposes a multi-energy storage system planning model to optimize the location and capacities, including battery and heat tanks, in regionally integrated energy systems in order to address the imbalance between renewable energy sources and user load. Ref. [20] also proposes a MESS planning optimization model considering power response characteristics of different storage media in integrated energy systems to realize capacity and types optimization.

Based on the previous study, this paper proposes a MESS planning model which aims to realize the optimal planning of short-term and long-term ESS in power system. The proposed MESS planning framework is formulated as a two-stage MILP model. The main contributions of this paper are summarized as follows:

- A MESS planning framework, including short-term ESS (battery energy storage) and long-term ESS (hydrogen energy storage) is proposed in this paper to address the risk of a mismatch between supply and demand on multiple time scales.
- The proposed planning framework of MESS is modeled as a two-stage stochastic MILP model based on typical scenarios. This allows the MESS planning results to adapt to the uncertainty of RES.
- The progressive hedging (PH) algorithm is used to solve the proposed model. Results demonstrate that the PH algorithm can boost computational efficiency under more scenarios.

The remainder of this paper is organized as follows. The planning framework of MESS is introduced in Section 2. The mathematical formulation of the MESS planning model

is established in Section 3. The PH algorithm is introduced in Section 4. The numerical experiments are presented in Section 5. Finally, conclusions of the full paper are drawn in Section 6.

2. Multi-Type Energy Storage Collaborative Optimization Planning Framework

HES and BES systems are often deployed together to leverage their strengths: HES provides long-term storage for seasonal shifts, while BES offers short-term grid stabilization and peak shaving. The structure of HES and BES in a power system is shown in Figure 1. An HES includes an electrolyser (P2H), hydrogen tank (HT) and fuel cell (FC). The storage scale of HES can be up to 1 million kilowatts and its duration time can be cross-seasonal. Cross-season regulation is particularly important in regions where there are long periods with minimal RES output (e.g., winters with low solar production). Hydrogen can be stored for months and converted back to electricity when needed, unlike battery systems that are more suited to short-term storage. For power systems, to mitigate the energy imbalance incurred by demand variations and seasonal fluctuation of RES, P2H uses the abundant electricity generated during off-peak periods to produce hydrogen with an electrolyser efficiency that is usually around 60–70%. The generated hydrogen is then stored in HT and, when the power supply is insufficient, fuel cells convert the stored hydrogen back into electricity. The conversion efficiency of fuel cells typically ranges from 40–60%. The efficiency and durability of FC and P2H will increase with ongoing advancements. BES, including many battery packs, typically uses lithium-ion (Li-ion) batteries due to their high energy density and fast response time. Li-ion batteries offer high round-trip efficiencies of around 85–95%, meaning only a small portion of energy is lost in charging and discharging cycles. The battery storage system is designed to discharge during peak load times, reducing the strain on the grid and avoiding the need for peaking power plants, which are typically fossil fuel based and less efficient. One of the key advantages of BES over HES is its ability to respond almost instantaneously to changes in demand or supply, making it invaluable for frequency regulation and for providing ancillary services to stabilize the grid. A collaborative approach between HES and BES enhances the grid's flexibility and resilience, allowing it to handle not just daily or weekly fluctuations, but also seasonal or extreme weather events that could severely disrupt supply.

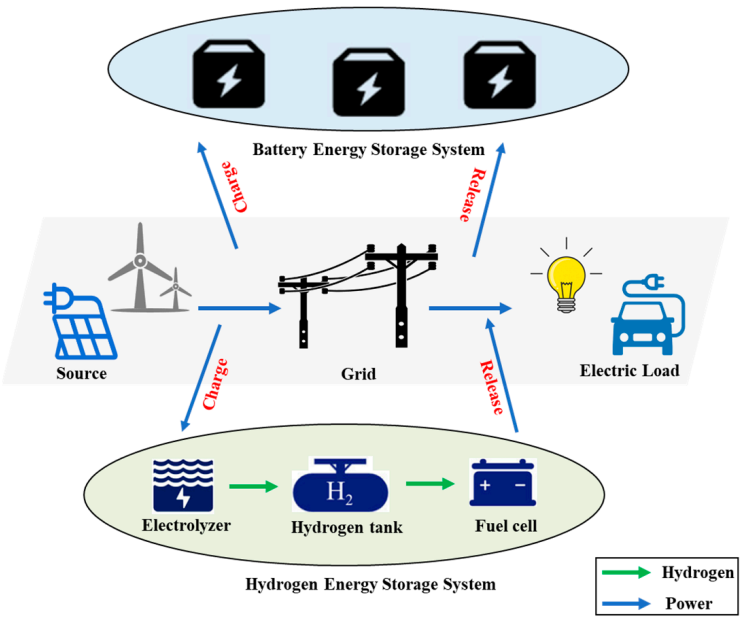

Figure 1. Conceptional structure of HES and BES in power system.

For short-term energy storage such as battery energy storage, since its duration time is short (2 h or 4 h) [21], its operation constraints need to meet a daily cycle and is modelled

based on typical days. However, for long-term energy storage such as hydrogen energy storage, since the duration time is usually longer [22], its operation constraints need to meet long-time scale cycle to keep the continuous dynamic change of hydrogen storage behavior. But 8760 h yearly data used in planning model may cause difficulty in model solution. Therefore, in this paper, yearly historical operation data are clustered by k-means algorithm. Different typical scenarios represent different seasons and based on the typical scenarios obtained by clustering, many similar repeated scenarios are replaced with typical scenarios, which can reduce the scale of the model and improve the computational efficiency.

Finally, to further consider the uncertainty of RES, this paper establishes the multi-type energy storage planning model by stochastic optimization method. Specifically, the first stage is to optimize the location and capacity of MESS and the second stage is to optimize system operation strategies under typical scenarios. The established MESS planning framework is shown in Figure 2.

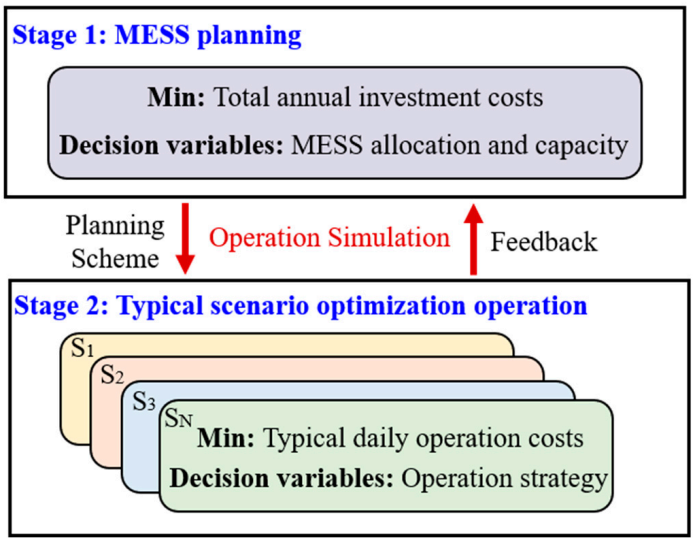

Figure 2. MESS planning framework.

3. Collaborative Optimization Planning Model

In this section, the proposed MESS collaborative optimization planning framework is formulated as a two-stage MILP model. The objective function of the planning model is as shown in (1). Specifically, the first stage optimizes the location and capacity of MESS including short-term ESS and long-term ESS, with the objective function of minimizing the investment cost. In the second stage, with the minimum operation cost as the objective function, the charging and discharging strategy of multi-type energy storage and the power system operation strategy are optimized based on the typical scenarios obtained by the clustering algorithm.

$$\min C_{ST\_inv} + C_{LT\_inv} + \sigma \sum p_r(s) C_{op}(s) \tag{1}$$

where, C_{ST_inv} is the total investment cost of short-term ESS. C_{LT_inv} is the total investment cost of long-term ESS. $p_r(s)$ is the typical scenario probability. $C_{op}(s)$ is the system operation cost under typical scenario s, including thermal unit generation cost and RES curtailment penalty. σ is the coefficient between equivalent annual cost and typical daily operation cost.

$$C_{ST\_inv} = \frac{r(1+r)^{T_i}}{(1+r)^{T_i}-1} \cdot \sum_{i \in \Omega_B} (C_{ess} H_S S_i^{ST} + C_{pss} S_i^{ST}) \tag{2}$$

$$C_{LT\_inv} = \frac{r(1+r)^{T_i}}{(1+r)^{T_i}-1} \cdot \sum_{i \in \Omega_H} C_{els} \frac{H_L S_i^{LT}}{LHV} + \frac{r(1+r)^{T_i}}{(1+r)^{T_i}-1} \cdot \sum_{i \in \Omega_H} 2 C_{pls} S_i^{LT} \tag{3}$$

$$C_{op}(s) = \sum_{g\in\Omega_G}\sum_{t\in T} c_g P^G_{g,t,s} + \sum_{i\in\Omega_W}\sum_{t\in T} c_w \Delta P^w_{i,t,s} \tag{4}$$

where, r is the discount rate; T_i is the life expectancy of different ESS; C_{ess} and C_{pss} are the investment cost of short-term ESS unit capacity and power, respectively; C_{els} and C_{pls} are the investment cost of long-term ESS unit capacity and power, respectively; S_i^{ST} and S_i^{LT} are short-term ESS configuration power and long-term ESS configuration power at the node i respectively; H_S is short-term ESS duration time (2 h in this paper) and H_L is long-term ESS duration time (720 h in this paper); LHV is the low heating value of hydrogen (kWh/kg H_2). c_g is the unit thermal generation cost; c_w is the unit RES power curtailment penalty cost; $P^G_{g,t,s}$ is the output of thermal unit g at time t under scenario s; $\Delta P^w_{i,t,s}$ is the RES curtailment of unit i at time t under scenario s.

3.1. ESS Investment and Planning Constraints

$$\sum_{i\in\Omega_B} x_i^S \le N_{ST} \tag{5}$$

$$\sum_{i\in\Omega_H} x_i^L \le N_{LT} \tag{6}$$

$$0 \le S_i^{ST} \le x_i^S S_{ST}^{\max} \tag{7}$$

$$0 \le S_i^{LT} \le x_i^L S_{LT}^{\max} \tag{8}$$

where, N_{ST} and N_{LT} are the maximum number of short-term ESS and long-term ESS allowed to be installed, respectively; x_i^S and x_i^L are binary variables indicating whether short-term ESS or long-term ESS are configured at node i. $S_{ST}^{\max}$ and $S_{LT}^{\max}$ are the maximum power allowed to be configured of short-term ESS and long-term ESS.

Constraints (5) and (6) limit the number of short-term and long-term ESS. Constraints (7) and (8) limit the capacity of short-term and long-term ESS.

3.2. Short-Term ESS Operation Constraints

$$0 \le P^{BC}_{i,t,s} \le u_{i,t,s} S_i^{ST} \tag{9}$$

$$0 \le P^{BD}_{i,t,s} \le (1-u_{i,t,s}) S_i^{ST} \tag{10}$$

$$SOC^{ST}_{i,t,s} = SOC^{ST}_{i,t-1,s} + P^{BC}_{i,t,s}\eta - P^{BD}_{i,t,s}/\eta \tag{11}$$

$$\mathrm{soc}_{\min} H_S S_i^{ST} \le SOC^{ST}_{i,t,s} \le \mathrm{soc}_{\max} H_S S_i^{ST} \tag{12}$$

$$SOC^{ST}_{i,0,s} = SOC^{ST}_{i,T,s} \tag{13}$$

where, $u_{i,t,s}$ is a binary variable indicating the charging and discharging state of short-term ESS i at time t under typical scenario s; $P^{BC}_{i,t,s}$ and $P^{BD}_{i,t,s}$ represent charging and discharging power of short-term ESS i at time t under typical scenario s, respectively; $SOC^{ST}_{i,t,s}$ is the capacity stored in short-term ESS i at time t under typical scenario s; $\mathrm{soc}_{\min}$ and $\mathrm{soc}_{\max}$ are the lower and upper limits of the state of charge.

Constraints (9) and (10) are short-term ESS charge and discharge constraints; Equation (11) describes the relationship of short-term ESS SOC between adjacent time in a typical day; Constraint (12) is SOC of short-term ESS limitation constraint. Equation (13) is SOC daily cycle constraint, indicating that SOC of short-term ESS at the initial time is as same as the end time [23].

3.3. Long-Term ESS Operation Constraints

$$SOC^L_{i,t+1,s} = SOC^L_{i,t,s} + \left(\frac{\eta^{\mathrm{Cha}} P^{\mathrm{HC}}_{i,t+1,s}}{LHV} - \frac{P^{\mathrm{HD}}_{i,t+1,s}}{\eta^{\mathrm{Dis}} LHV}\right) \tag{14}$$

$$SOC_{i,1,s}^{L} = SOC_{i,T,s-1}^{L} + (\frac{\eta^{\mathrm{Cha}} P_{i,1,s}^{\mathrm{HC}}}{LHV} - \frac{P_{i,1,s}^{\mathrm{HD}}}{\eta^{\mathrm{Dis}} LHV}) \tag{15}$$

$$SOC_{i,1,1}^{L} = SOC_{i,T,4}^{L} \tag{16}$$

$$0 \le P_{i,t,s}^{\mathrm{HC}}, P_{i,t,s}^{\mathrm{HD}} \le S_i^{LT} \tag{17}$$

$$\mathrm{soc}_{\min} H_L S_i^{LT} \le LHV \cdot SOC_{i,t,s}^{LT} \le \mathrm{soc}_{\max} H_L S_i^{LT} \tag{18}$$

where, $SOC_{i,t,s}^{L}$ represents SOC component of long-term ESS i at time t under typical scenario s, $P_{i,t,s}^{HC}$ and $P_{i,t,s}^{HD}$ represent charging and discharging power of long-term ESS i at time t under typical scenario s, respectively.

Equations (14) and (15) describes the SOC component relationship of long-term ESS between adjacent days [24]. Equation (16) are SOC cycle constraints, indicating the initial and final SOC should be equal. Equation (17) is long-term ESS charge and discharge constraints. Equation (18) is SOC of long-term ESS limitation constraint.

3.4. Generators Operation Constraints

$$P_g^{\min} \le P_{g,t,s}^{G} \le P_g^{\max} \tag{19}$$

$$-R_g^{U} \le P_{g,t,s}^{G} - P_{g,t-1,s}^{G} \le R_g^{U} \tag{20}$$

$$0 \le \Delta P_{i,t,s}^{w} \le P_{i,t,s}^{w} \tag{21}$$

where, $P_g^{\min}$ and $P_g^{\max}$ is the maximum and minimum allowable output power of thermal unit g. R_g^{U} is maximum allowable ramping power; $P_{i,t,s}^{w}$ is the output power of RES unit i at time t under typical scenario s.

Constraint (19) is the output power limitation constraint of the thermal unit. Constraint (20) is the flexible ramping constraint [10]. Constraint (21) is RES power curtailment constraint.

3.5. Power System Operation Constraints

$$\begin{aligned} &\sum_{i\in\Omega_G} P_{i,t,s}^{G} + \sum_{i\in\Omega_W} (P_{i,t,s}^{W} - \Delta P_{i,t,s}^{W}) + \sum_{l\in\Omega_i^{LE}} P_{l,t,s} - \sum_{l\in\Omega_i^{LS}} P_{l,t,s} \\ &+ \sum_{i\in\Omega_B} (P_{i,t,s}^{BD} - P_{i,t,s}^{BC}) + \sum_{i\in\Omega_H} (P_{i,t,s}^{HD} - P_{i,t,s}^{HC}) = P_{i,t,s}^{Load} \end{aligned} \tag{22}$$

$$P_{l,t,s} = (\sum_{i\in\Omega_l^{LS}} \theta_{i,t,s} - \sum_{j\in\Omega_l^{LE}} \theta_{j,t,s})/x_l \tag{23}$$

$$-P_l^{\max} \le P_{l,t,s} \le P_l^{\max} \tag{24}$$

$$\theta_i^{\min} \le \theta_{i,t,s} \le \theta_i^{\max} \tag{25}$$

where, $P_{l,t,s}$ is the transmission power of line l at time t under typical scenario s; $P_{i,t,s}^{Load}$ is the load demand of node i at time t under typical scenario s, $\theta_{i,t,s}$ is the node phase angle of node i at time t under typical scenario s; x_l is the reactance of line l; $P_l^{\max}$ is the allowable maximum power of line l, $\theta_i^{\min}$ and $\theta_i^{\max}$ are allowable minimum and maximum phase angle.

Equation (22) is power balance constraints. Equation (23) is the transmission line power flow constraint based on DC power flow [25]. Constraint (24) is the constraint on the maximum transmission power of a transmission line. Constraint (25) is the constraint on the allowable range of node phase angles. Note that the DC power flow is used in this paper to describe the operating constraints of transmission systems, which is based on the following assumptions: (1) the voltage of each bus of the power system is usually near the rated voltage; (2) The phase angle difference between the two ends of the line is very small.

4. Solution Algorithm

The proposed MESS collaborative optimization planning framework in this paper is formulated as a scenario-based two-stage stochastic mixed integer linear optimization program model. In this section, PH algorithm is applied to realize the efficiency solving of the proposed model. The compact form of the two-stage stochastic program proposed in this paper is shown in (26) and (27):

$$\min_{x,y}\left\{c^{\mathrm{T}}x+\sum_{s}p(s)(f_s^{\mathrm{T}},y_s)\right\} \tag{26}$$

$$\text{s.t.}\begin{cases} Ax\le b \\ Cy_s\le d(s)-e(s)x \end{cases} \tag{27}$$

where x represents investment and planning decision variables, which are scenario independent. y_s represents the second-stage operation decision variables based on scenarios.

For the first stage problem, decision variable x does not depend on stochastic parameters, which is obtained before the realization of stochastic parameters. The second stage problem depends on stochastic parameters, decision variable y_s is obtained after the realization of stochastic parameters. PH algorithm decomposes the main problem to several sub-problems with respect to scenarios, as shown in (28)–(30).

$$\min_{x,y}\left\{\sum_{s\in S}c^{\mathrm{T}}x(s)+\sum_{s\in S}p(s)(f_s^{\mathrm{T}},y_s)\right\} \tag{28}$$

$$\text{s.t.}\begin{cases} Ax\le b \\ Cy_s\le d(s)-e(s)x \end{cases} \tag{29}$$

$$\text{s.t. } x(1)=x(2)=\ldots=x(S) \tag{30}$$

where $x(1)=x(2)=\ldots=x(S)$ represents the non-anticaptivity constraint [26], due to the non-anticaptivity constraint, all realizations $x(i)$ of the first-stage decisions are equal, that is, they do not depend on the realization of stochastic parameters. In other words, non-anticaptivity constraint in (30) stipulates the first-stage decision variable x to be independent of scenarios [27,28]. As shown in Figure 3, Formulations (28)–(30) slip the two-stage stochastic program model (a) into scenario-based sub-problems with non-anticaptivity constraints (b).

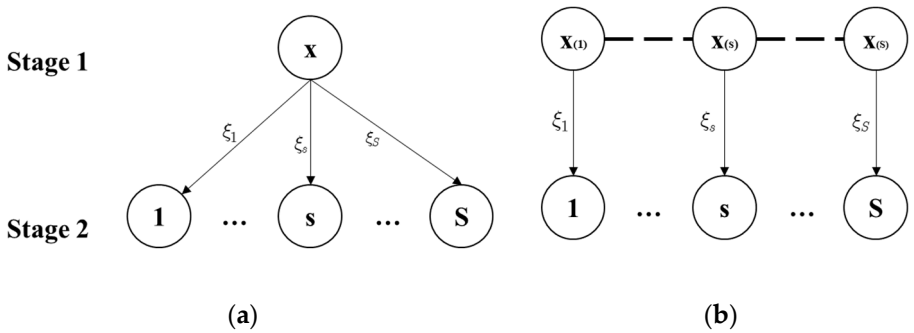

Figure 3. (**a**) Scenario tree for two-stage stochastic program; (**b**) Scenarios with non-anticaptivity constraints.

The specific solving process of PH algorithm is shown in Algorithm 1 of the manuscript. Careful attention of the penalty coefficient ρ is given to enhance the efficiency and accuracy of the PH algorithm in the proposed model, in this paper, the penalty coefficient ρ is set according to [26].

Algorithm 1. Progressive Hedging (PH) Algorithm.

Step 1 Initialization:
Set $k = 0, w^k(s) = 0$
for $s = 1 : S$
$x^{k=0}(s) = \underset{x(s)}{\operatorname{argmin}}\{c^{\mathrm{T}}x(s) + f_s^{\mathrm{T}}y_s\}$
end
$\overline{x} = \sum_{s\in S} p(s)x^{k=0}(s)$
Step 2 Iteration update:
$k = k + 1$
Step 3 Update multiplier and decomposition:
for $s = 1 : S$ do
$w^k(s) = w^{k-1}(s) + \rho\cdot(x^{k-1}(s) - \overline{x})$
$x^k(s) = \underset{x(s)}{\operatorname{argmin}}\left\{c^{\mathrm{T}}x(s) + f_s^{\mathrm{T}}y_s + w^k(s)\cdot x(s) + \frac{\rho}{2}\|x(s) - \overline{x}\|^2\right\}$
end
$\overline{x} = \sum_{s\in S} p(s)x^k(s)$
$\varepsilon^k = \sum_{s\in S} p(s)\cdot\|x^k(s) - \overline{x}\|^2$
Step 4 Termination:
If $\varepsilon^k <$ gap : Stop and return $x^k(s)$
Else go to Step 2 and continue

5. Case Study

5.1. Test System Introduction

In this paper, the modified IEEE 39-bus system [29] is used to validate the effectiveness of the proposed planning model. The system topology is shown in Figure 4, the system has 39 nodes, 10 conventional thermal power units and 46 transmission lines. In order to simulate the situation of RES, the system is connected to three groups of wind farms, located at nodes 33, 34 and 35 respectively. The installed capacity of thermal power is 6500 MW, the installed capacity of wind power is 3000 MW, the maximum load of the system is 6200 MW, the minimum load is 4500 MW. Based on the yearly RES power output scenarios, the typical scenarios are reduced by K-means clustering algorithm [30]. Cost parameters can be found in [31]. The program was performed by Matlab and Yalmip, and was solved by Gurobi under the default settings.

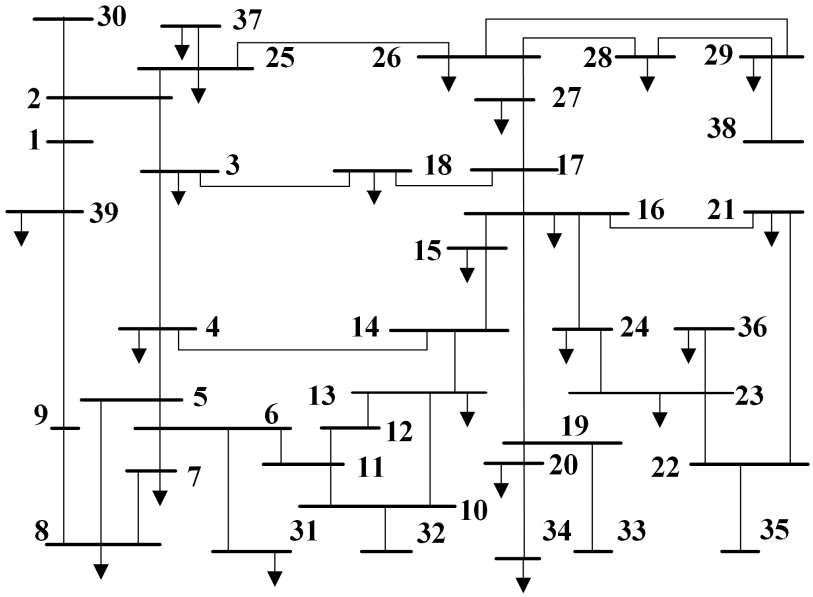

Figure 4. Modified IEEE 39-bus system.

5.2. MESS Planning Results

This section shows the optimization results of the multi-type energy storage collaborative planning model proposed in this paper. Tables 1 and 2 show the optimization planning results of battery energy storage and hydrogen energy storage respectively.

Table 1. Battery energy storage planning results.

Node	Power (MW)	Capacity (MWh)
15	86.03	172.06
17	94.8	189.6
20	13.83	27.66
32	37.87	75.74
Total	232.53	465.06

Table 2. Hydrogen energy storage planning results.

Node	Power (MW)	Capacity (t H_2)
30	100	2400
34	10.15	243.6
36	167.54	4020.96
Total	277.69	6664.56

The total installed battery energy storage power is 232.53 MW and the capacity is 465.06 MWh. Node 15, 17, 20 and 32 are configured with 86.03/172.06, 94.8/189.6, 13.83/27.66, 37.87/75.74 MW/MWh energy storage. The total installed hydrogen storage power is 277.69 MW and the capacity is 6664.56 t hydrogen storage tanks, which are respectively located at nodes 30, 34 and 36.

5.3. MESS Operation Strategy Results

This section further analyzes the operation strategies of different types of energy storage in power system. Operation strategy of battery energy storage and hydrogen energy storage are shown in Figures 5 and 6.

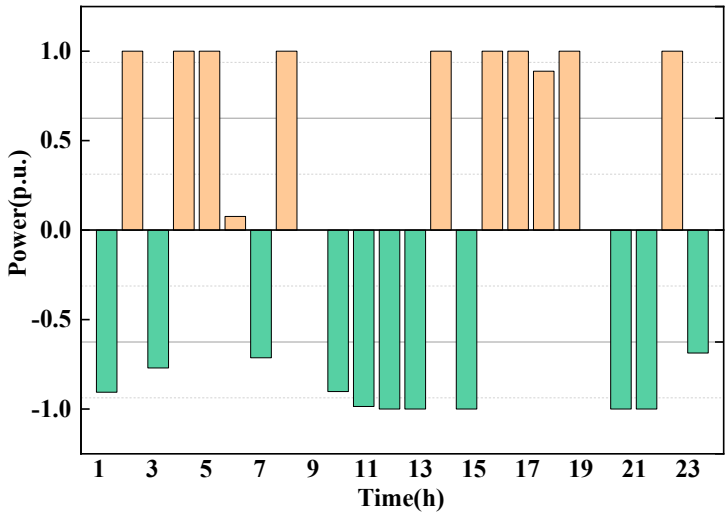

Figure 5. Operation strategy of battery energy storage.

Due to intra-daily SOC cycle constraints, the main role of battery energy storage is to provide intra-day flexible regulation capacity to achieve efficient consumption of renewable energy. Specifically, battery energy storage discharge during the load peak and charge during the load off-peak. In conclusion, reasonable planning of battery energy storage can improve intra-day peak regulation capacity.

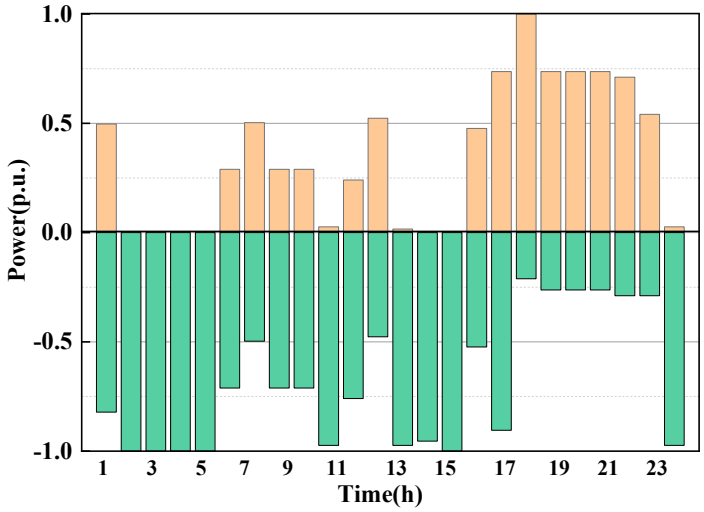

Figure 6. Operation strategy of hydrogen energy storage.

In addition, the hydrogen energy storage operation strategy on typical day 1 (spring) is shown in Figure 6. The operation strategy of hydrogen energy storage is different in different seasons. The charging power of hydrogen energy storage is greater than that of discharge in the season when the renewable energy output is large (spring). In conclusion, reasonable planning of hydrogen energy storage can improve renewable energy seasonal fluctuation. So, for power system, it is necessary to achieve the dynamic time–delay balance of supply and demand through the coordination of multiple types of energy storage to address the risk of multi-time scale supply and demand imbalance caused by the high proportion of renewable energy access.

5.4. Proposed Model and Algorithm Efficiency

This section verifies the efficiency of the proposed stochastic optimization model and PH algorithm.

Firstly, the validity of the stochastic optimization (SO) model is verified by comparing it with the robust optimization (RO) model and the distributionally robust optimization (DRO) model, as shown in Table 3. The uncertain set modeling method of RO is the same as that of Reference [32], while the ambiguity set modeling method of DRO is the same as that of Reference [33]. It can be found that the planning cost of SO is lower than that of RO. This is because RO is planning for the worst scenario, and the probability of this worst scenario is generally small, so the planning scheme obtained by RO is often too conservative, resulting in a waste of resources; In other words, SO can avoid the disadvantage of RO being too conservative. On the other hand, the planning scheme obtained by DRO is close to that obtained by SO, but the solving time of SO is significantly reduced, which shows that the proposed SO achieves a balance between effectiveness and solving speed.

Table 3. Comparison of optimization results of SO, RO and DRO.

Model	Short-Term ESS Planning Result	Long-Term ESS Planning Result	Solving Time
SO	232.53 MW/465.06 MWh	277.69 MW/6664.56 t H_2	126 s
RO	326.59 MW/692.38 MWh	344.36 MW/8635.19 t H_2	682 s
DRO	248.51 MW/513.09 MWh	288.96 MW/7069.87 t H_2	2153 s

Besides, two solving methods, PH algorithm and directly solving by Gurobi, is firstly compared in this section. The solving time is shown in Table 4. N/A represents that the planning model cannot find a solution within 10,000 s. Firstly, 4 typical scenarios including spring, summer, autumn, winter are applied to compare the PH algorithm efficiency. The

solving time of directly solving by Gurobi is less than PH algorithm. With the increase of the number of scenarios, the solving efficiency of the PH algorithm gradually appears. The PH algorithm can improve the solving efficiency by solving the second-stage operation sub-problems in parallel. When the number of scenarios is 16 (4 typical scenarios in spring, summer, autumn and winter), the solution time of both is basically the same. With the further increase in the number of scenarios, the solution time of PH algorithm is less than that of the direct solution. When the number of scenarios is 128, the result cannot be obtained within the effective time (10,000 s) by direct solution, but the solution of the model can still be efficiently obtained by PH algorithm. So, PH algorithm can realize the efficiency solution of the proposed model in this paper under larger scenarios.

Table 4. Solving efficiency of PH algorithm.

Scenarios Number	PH Algorithm	Directly Solving by Gurobi
4	126 s	86 s
8	194 s	161 s
16	452 s	450 s
64	1634 s	2608 s
128	4259 s	N/A

In order to further illustrate the effectiveness of the proposed method, this paper verifies the validity of the PH algorithm in IEEE 300-bus system. The system consists of 69 thermal power units, 411 lines, and 8 wind farms. Specific information of IEEE 300-bus system can be found in [34]. Table 5 compares solving efficiency of PH algorithm in IEEE 39-bus system and IEEE 300-bus system, the results show that PH algorithm is still efficient in large network by parallel computations. Therefore, the multi-type energy storage collaborative planning framework and solution method proposed in this paper can meet the practical engineering needs.

Table 5. Solving efficiency of PH algorithm in 39-bus system and 300-bus system.

Scenarios Number	IEEE 39-Bus System	IEEE 300-Bus System
4	126 s	232 s
8	194 s	361 s
16	452 s	708 s
64	1634 s	2793 s
128	4259 s	7693 s

6. Conclusions

This paper proposes a multiple types energy storage collaborative optimization planning model to address the risk of multi-time scale supply and demand imbalance due to a high proportion of renewable energy. To reduce the model scale and improve computational efficiency, the planning model is established as a typical scenario-based two-stage MILP model and the PH algorithm is introduced to solve the proposed MILP model based on scenarios. The location and capacity of short-term energy storage and long-term energy storage are optimized in the first stage; power system operation strategies are optimized in the second stage.

The model is tested on the modified IEEE-39 bus system. Results indicate that the proposed multiple types of energy storage collaborative optimization planning model can realize battery energy storage and hydrogen energy storage optimization allocation in power system. PH algorithm can realize the efficient solution of the proposed model by parallel solving and is more efficient with the growing number of scenarios. Compared with the existing methods, the economy of energy storage planning results is further improved.

In future studies, we will further study the combination of long-term weather prediction model and energy storage planning model, as well as the energy storage planning method considering the hydrogen industry chain.

Author Contributions: Conceptualization, Y.Y.; methodology, Y.Y. and Q.L.; validation, Z.Y. and W.W.; formal analysis, W.W.; investigation, Q.H.; resources, Z.Y.; data curation, Q.L. All authors have read and agreed to the published version of the manuscript.

Funding: This work is supported by the Science and Technology Project of China Southern Power Grid Corporation. (Project No. 036000KK52220025 (GDKJXM20220329)).

Data Availability Statement: The data presented in this study are available on request from the corresponding author due to (specify the reason for the restriction).

Acknowledgments: We would like to express our gratitude to all the reviewers for providing valuable feedback.

Conflicts of Interest: The authors declare no conflicts of interest.

References

1. Agency IRE. World Energy Transitions Outlook: 1.5 °C Pathway. 2021. Available online: https://www.irena.org/Energy-Transition/Outlook (accessed on 24 July 2024).
2. EPRI Head: Duck Curve Now Looks like a Canyon. 2023. Available online: https://www.powermag.com/epri-head-duck-curve-now-looks-like-a-canyon/ (accessed on 24 July 2024).
3. Petkov, I.; Gabrielli, P. Power-to-hydrogen as seasonal energy storage: An uncertainty analysis for optimal design of low-carbon multi-energy systems. *Appl. Energy* **2020**, *274*, 115197. [CrossRef]
4. Sun, Y.; Zhao, Z.; Yang, M.; Jia, D.; Pei, W.; Xu, B. Overview of energy storage in renewable energy power fluctuation mitigation. *CSEE J. Power Energy Syst.* **2020**, *6*, 160–173.
5. Revinova, S.; Lazanyuk, I.; Gabrielyan, B.; Shahinyan, T.; Hakobyan, Y. Hydrogen in Energy Transition: The Problem of Economic Efficiency, Environmental Safety, and Technological Readiness of Transportation and Storage. *Resources* **2024**, *13*, 92. [CrossRef]
6. Agency IEA. Electricity Market Report 2023—Analysis. 2023. Available online: https://iea.blob.core.windows.net/assets/255e9cba-da84-4681-8c1f-458ca1a3d9ca/ElectricityMarketReport2023.pdf. (accessed on 24 July 2024).
7. Wang, C.; Zhang, X.; Xia, Y.; Xiong, H.; Guo, C.; Wang, L.; Wang, Y. A two-stage robust optimal configuration model of generation-side cloud energy storage system based on cooperative game. *IET Gener. Transm. Distrib.* **2022**, *17*, 1723–1733. [CrossRef]
8. Zhang, Z.; Zhang, X.; Duan, N.; Pengjiang, G.; Jinli, L.; Wenzhuo, W.; Ying, W. The Synergistic and Optimal Configuration of Energy Storage and Renewable Energy Based on the Equal Area Principle. *Power Syst. Technol.* **2023**, *47*, 4131–4142. (In Chinese)
9. Zhu, X.; Shan, Y. Multi-stage distributionally robust planning of energy storage capacity considering flexibility. *Electr. Power Autom. Equip.* **2023**, *43*, 152–159+167. (In Chinese)
10. Tang, S.; Li, G.; Wang, Z.; Yang, Y.; Lu, Q.; Xie, P.; Chen, Y. A Distributionally Robust Energy Storage Planning Model for Wind Integrated Power System Based on Scenario Probability. In Proceedings of the 2023 International Conference on Power Energy Systems and Applications (ICoPESA), Nanjing, China, 20–22 June 2023; pp. 554–560.
11. Fu, P.; Pudjianto, D.; Zhang, X.; Strbac, G. Integration of Hydrogen into Multi-Energy Systems Optimisation. *Energies* **2020**, *13*, 1606. [CrossRef]
12. Luo, W.; Wu, J.; Cai, J.; Mao, Y.; Chen, S. Capacity Allocation Optimization Framework for Hydrogen Integrated Energy System Considering Hydrogen Trading and Long-Term Hydrogen Storage. *IEEE Access* **2023**, *11*, 15772–15787.
13. Li, J.; Li, G.; Ma, S.; Liang, Z.; Li, Y.; Zeng, W. Modeling and Simulation of Hydrogen Energy Storage System for Power-to-gas and Gas-to-power Systems. *J. Mod. Power Syst. Clean Energy* **2021**, *11*, 885–895. [CrossRef]
14. Xiong, Y.; Chen, L.; Zheng, T.; Si, Y.; Mei, S. Electricity-Heat-Hydrogen Modeling of Hydrogen Storage System Considering Off-Design Characteristics. *IEEE Access* **2021**, *9*, 156768–156777. [CrossRef]
15. Lu, Q.; Zhang, X.; Yang, Y.; Hu, Q.; Wu, G.; Huang, Y.; Liu, Y.; Li, G. Multi-Time-Scale Energy Storage Optimization Configuration for Power Balance in Distribution Systems. *Electronics* **2024**, *13*, 1379. [CrossRef]
16. Du, E.; Jiang, H.; Xiao, J.; Hou, J.; Zhang, N.; Kang, C. Preliminary analysis of long-term storage requirement in enabling high renewable energy penetration: A case of East Asia. *IET Renew. Power Gener.* **2021**, *15*, 1255–1269. [CrossRef]
17. Jiang, S.; Wen, S.; Zhu, M.; Huang, Y.; Ye, H. Scenario-Transformation-Based Optimal Sizing of Hybrid Hydrogen-Battery Storage for Multi-Timescale Islanded Microgrids. *IEEE Trans. Sustain. Energy* **2023**, *14*, 1784–1795. [CrossRef]
18. Wu, X.; Cao, B.; Liu, B.; Wang, X. A Planning Model of Standalone Hydrogen-Based Carbon-Free Microgrid through Convex Relaxation. *IEEE Trans. Smart Grid* **2023**, *14*, 2668–2680. [CrossRef]
19. Wang, J.; Deng, H.; Qi, X. Cost-based site and capacity optimization of multi-energy storage system in the regional integrated energy networks. *Energy* **2022**, *261*, 125240. [CrossRef]

20. Gao, M.; Han, Z.; Zhao, B.; Li, P.; Wu, D.; Li, P. Optimal planning method of multi-energy storage systems based on the power response analysis in the integrated energy system. *J. Energy Storage* **2023**, *73*, 109015. [CrossRef]
21. Luo, Y.; Tian, P.; Yan, X.; Xiao, X.; Ci, S.; Zhou, Q.; Yang, Y. Energy Storage Dynamic Configuration of Active Distribution Networks—Joint Planning of Grid Structures. *Processes* **2024**, *12*, 79. [CrossRef]
22. Alharthi, Y.Z. An Analysis of Hybrid Renewable Energy-Based Hydrogen Production and Power Supply for Off-Grid Systems. *Processes* **2024**, *12*, 1201. [CrossRef]
23. Yan, C.; Geng, X.; Bie, Z.; Xie, L. Two-stage robust energy storage planning with probabilistic guarantees: A data-driven approach. *Appl. Energy* **2022**, *313*, 118623. [CrossRef]
24. Pan, G.; Gu, W.; Lu, Y.; Qiu, H.; Lu, S.; Yao, S. Optimal Planning for Electricity-Hydrogen Integrated Energy System Considering Power to Hydrogen and Heat and Seasonal Storage. *IEEE Trans. Sustain. Energy* **2020**, *11*, 2662–2676. [CrossRef]
25. Chen, Y.; Hu, Q.; Lin, X.; Lu, Q.; Zhu, Y.; Li, G. Energy Storage Stochastic Optimization Planning Considering Dynamic Frequency Constraints. In Proceedings of the 2023 2nd Asia Power and Electrical Technology Conference (APET), Shanghai, China, 28–30 December 2023; pp. 828–833.
26. Watson, J.-P.; Woodruff, D.L. Progressive hedging innovations for a class of stochastic mixed-integer resource allocation problems. *Comput. Manag. Sci.* **2010**, *8*, 355–370. [CrossRef]
27. Shapiro, A.; Dentcheva, D.; Ruszczynski, A. *Lectures on Stochastic Programming: Modeling and Theory*; SIAM: Philadelphia, PA, USA, 2014.
28. Popela, P.; Novotný, J.; Roupec, J.; Hrabec, D.; Olstad, A. Two-stage Stochastic Programming for Engineering Problems. *Eng. Mech.* **2014**, *21*, 335–353.
29. Illinois. IEEE 39-Bus System [EB/OL]. Available online: https://icseg.iti.illinois.edu/ieee-39-bus-system (accessed on 2 November 2023).
30. Hu, Q.; Li, G.; Sun, S.; Bie, Z. Incorporating catastrophe insurance in power distribution systems investment and planning for resilience enhancement. *Int. J. Electr. Power Energy Syst.* **2024**, *155*, 109438. [CrossRef]
31. Lu, J.; Li, X. Annual Benefit Analysis of Integrating the Seasonal Hydrogen Storage into the Renewable Power Grids. In Proceedings of the 2023 IEEE Power & Energy Society General Meeting (PESGM), Orlando, FL, USA, 16–20 July 2023; pp. 1–5.
32. Zhang, Z.; Guo, Z.; Zhou, M.; Wu, Z.; Yuan, B.; Chen, Y.; Li, G. Equalizing multi-temporal scale adequacy for low carbon power systems by co-planning short-term and seasonal energy storage. *J. Energy Storage* **2024**, *84*, 111518. [CrossRef]
33. Chen, C.; Xing, J.; Li, Q.; Liu, S.; Ma, J.; Chen, J.; Han, L.; Qiu, W.; Lin, Z.; Yang, L. Wasserstein distance-based distributionally robust optimal scheduling in rural microgrid considering the coordinated interaction among source-grid-load-storage. *Energy Rep.* **2021**, *7*, 60–66. [CrossRef]
34. Teng, M.; Chen, C.; Zhao, Y.; Zhong, J.; Geng, J.; Lv, J.; Bie, Z. Distribution Robust Optimal Day-ahead Dispatch Method for Power Systems with Uncertain Wind Power Access Considering Deep Peak Regulation of Coal-fired Units and Energy Storage. *Power Syst. Technol.* **2024**, *48*, 3122–3132. (In Chinese)